Available online at www.sciencedirect.com
SciVerse ScienceDirect
Ceramics International xxx (2011) xxx–xxx
CERAMICS INTERNATIONAL
www.elsevier.com/locate/ceramint

Dense zircon ($ZrSiO_4$) ceramics by high energy ball milling and spark plasma sintering

Nicolas M. Rendtorff [a,b,c,*], Salvatore. Grasso [c], Chunfeng Hu [c,d], Gustavo Suarez [a,b], Esteban F. Aglietti [a,b], Yoshio Sakka [c,d]

[a] Centro de Tecnologia de Recursos Minerales y Cerámica (CETMIC): (CIC-CONICET-CCT La Plata), Camino Centenario y 506, C.C. 49, M.B. Gonnet, B1897ZCA Buenos Aires, Argentina
[b] Facultad de Ciencias Exactas, Universidad Nacional de La Plata, 47 y 115 La Plata, Buenos Aires, Argentina
[c] Fine Particle Processing Group, Nano Ceramics Center, National Institute for Materials Science (NIMS), 1-2-1 Sengen, Tsukuba, Ibaraki 305-0047, Japan
[d] WPI-MANA World Premier International Research Center Initiative, Center for Materials Nanoarchitectonics, NIMS, 1-2-1 Sengen, Tsukuba, Ibaraki 305-0047, Japan

Received 2 June 2011; received in revised form 30 September 2011; accepted 1 October 2011

Abstract

The addition of sintering additives has always been detrimental to the mechanical properties of sintered ceramics; therefore, methods to reduce or, as in this case, eliminate sintering additives are usually relevant. In this paper, dense zircon ceramics were obtained starting from mechanically activated powder compacted by spark plasma sintering without employing sintering additives.

The high energy ball milling (HEBM) of starting powder was effective to enhance the sintering kinetics. The structural changes of the zircon powder introduced by the HEBM were evaluated. The phase composition and the microstructure of bulk zircon material were analyzed by SEM (EDAX) and XRD. The Vickers hardness and the fracture toughness were evaluated as well.

Fully dense materials were obtained at 1400 °C with a heating rate of 100 °C/min, 10 min soaking time and 100 MPa uniaxial pressure. The zircon samples sintered at temperatures above 1400 °C were dissociated in monoclinic zirconia and amorphous silica. The dissociation was detrimental for the mechanical properties. Unlike conventional sintering methods (hot pressing, pressureless sintering) SPS permitted to overcome the dissociation of the zircon material and to obtain additive free, fully dense zircon ceramic with outstanding mechanical properties.

Keywords: A. Sintering; Zircon; High energy milling; SPS

1. Introduction

Zircon ($ZrSiO_4$) is an abundant raw material, with moderately low thermal linear expansion (4.10^{-6} °C^{-1}) and very high chemical inertness even in contact with glassy phase and molten slag. It has been demonstrated that high purity zircon can retain its bending strength up to temperatures as high as 1200–l400 °C [1–5]. Owing to these properties, zircon-dense bodies have being considered as excellent candidates for structural applications in severe conditions (i.e. continuous steel casting, glass fiber technology, etc.) [6,7].

Due to its refractoriness, it is difficult to obtain fully dense zircon ceramics. The employed sintering aids like TiO_2 [8], SiO_2 [9] and Al_2O_3 [10] contribute to lower the high temperature mechanical properties and chemical inertness.

The highly abundant natural zircon sand is the principal source for zircon materials. However natural zircon sand often contains several impurities which influence the final properties of these materials. Several investigations have attempted to obtain pure zircon powder via sol–gel routes [1,11–15], chemical reactions like aerosols [16], reverse micelle process [17] and micro-emulsion process [18]. The method based on the mixture of amorphous ZrO_2–SiO_2 revealed the incomplete powders crystallization under heat treatment [19,20] or laser [21].

* Corresponding author at: Centro de Tecnologia de Recursos Minerales y Cerámica (CETMIC): (CIC-CONICET-CCT La Plata), Camino Centenario y 506, C.C. 49, M.B. Gonnet, B1897ZCA Buenos Aires, Argentina.
Tel.: +54 221 4840247; fax: +54 221 4710075.
E-mail address: rendtorff@cetmic.unlp.edu.ar (N.M. Rendtorff).

0272-8842/$36.00
doi:10.1016/j.ceramint.2011.10.001

Zircon dissociation mechanism, recently reviewed in Ref. [22], is influenced by the impurity content. It has been demonstrated that the onset dissociation temperature is decreases with the impurities content. At temperature over 1650 °C, the products of zircon dissociation are tetragonal zirconia and fused silica; however, the presence of impurities like TiO_2, FeO_x and/or alkali lowers the dissociation temperature by about 200 °C [22,23]. During the cooling the tetragonal zirconia resulting from the zircon dissociation might transform into monoclinic zirconia which is the stable phase at room temperature. It is well known the phase transformation is accompanied by a significant volume change which introduces microcracks inside the zirconia particles, dispersed into the ceramic matrix [24–26], thus, resulting in a detrimental effect on the mechanical properties. On the other hand, the resulting silica from the zircon dissociation might also decrease both the high temperature mechanical properties and the chemical inertness.

The mechanochemical activation process has proved to be an effective technique to enhance a solid-state reaction at room temperature [27]. The ''mechanical'' effects of milling, such as the reduction of particle size and mixture homogenization, are combined with chemical effects, such as partial decomposition of salts or hydroxides, thus, resulting in active reactants with high surface energy. Recently Antsiferov et al. reported that mechanical activation of zircon materials [28] was obtained after a preliminary mechanical activation process. Under low energy milling conditions, the authors showed the benefits of dry treatments over instead of wet treatments. However, at temperature as high as 1600 °C the relative density was below 95%. The milling pretreatment was investigated in the case of zircon materials obtained by the reaction sintering of SiO_2 and ZrO_2 [29].

In order to overcome the dissociation problems we attempted to obtain fully dense zircon ceramics starting from high energy ball milled powder followed by SPS at low temperature (i.e. 1400 °C) and short time sintering (i.e. 10 min) [30–35]. Unlike conventional methods (i.e., pressureless sintering, hot-pressing), the current activated sintering methods, as spark plasma sintering (SPS), permits to lower sintering temperature and shorten the holding time. As result, the SPS leads to remarkable improvements in properties of consolidated materials. The low SPS temperatures and short holding times enable the densification of nanometric powders to near theoretical values with limited grain growth [30–35].

The aims of the present work are: to obtain fully dense zircon materials from commercially available powders and to avoid the zircon thermal dissociation by combination of high-energy ball-milling (HEBM) pretreatment and spark plasma sintering (SPS) technique.

2. Experimental procedures

The starting powder was with zirconium silicate with ZrO_2 = 64–65.5 wt%, SiO_2 = 33–34 wt%, $Fe_2O_3 \leq 0.10$ wt% and $TiO_2 \leq 0.15$ wt%, mean diameter (D_{50}) of 1.5 μm, specific gravity of 4.6 g/cm^3, melting point of 2200 °C and hardness (Mohs) of 7.5 (Kreutzonit Super, Mahlwerke Kreutz, Germany).

The mechanochemical activation of the zircon powder was performed in dry milling conditions using a high energy planetary mill (7 Premium Line, Fritsch Co., Ltd., Germany). In order to minimize contamination during the HEBM, the jar and milling media employed were made of zirconia; 85 ml zirconia jars were used with 60 g of zirconia balls (3 mm diameter) as milling media; the ratio between the weight of powder and the milling balls was 1:10 in each batch [27]. A 900 rpm speed was used: in these conditions the milling is so energetic that the jars were left to cool down for 90 min after 5 min HEBM. Particle size distribution for the powders milled for different times was measured with a Laser Diffraction Particle Size Distribution Analyzer (Horiba LA-300; ASTM D 4464-00).

Densification of the ball-milled powders was conducted using a SPS machine (SPS-1050, Sumitomo, Kawasaki, Japan). Fig. 1 shows a schematic drawing of the SPS device showing its main constitutive units. The powder was poured into a graphite die with an inner diameter of 10 mm. In a typical sintering experiment, 1.0 g of milled zircon powder was poured into the die. The temperature was measured accurately using a pyrometer focused on the die surface of the inner die (i.e., 1 cm far from the sample edge). Graphite felt was used to reduce the heat loss by radiation. The powder was heated from room temperature up to 700 °C for 10 min, subsequently, up to the sintering temperature (1200, 1300, 1400 and 1500 °C) with a constant heating rate of 100 °C/min. Depending on the sintering temperature, samples were named S12, S13, S14 and S15 respectively. The dwell time was 10 min and 100 MPa pressure was raised just after the beginning of the dwell time. In order to achieve full dense sample at lower sintering temperature, different longer dwell time (between 10 and 60 min) were also attempted. Heating was conducted using a sequence consisting of 12 DC pulses (40.8 ms) followed by zero current for 6.8 ms. During the entire duration of the experiments, the electric current intensity was below 1000 A and the voltage drop between the cooled rams was below 4 V. Density and apparent porosity of the sintered samples were evaluated by the Archimedes method.

The phase composition of the ball-milled powders and the sintered specimens was determined by X-ray diffraction (XRD) using CuKα radiation operating at 40 kV and 300 mA. The microstructural observations were conducted by scanning electron microscopy (SEM) (Joel, JSM-6500F, Japan). The surfaces of the specimens were polished with diamond slurries of 15, 9, 6, 3, 1 and 0.25 μm particle sizes.

Vickers hardness (Hv) and fracture toughness (K_{IC}) of the obtained ceramics were evaluated with a Vickers indentation machine (Akashi AVK-A, Japan): at least six indents under 5 kg of load were performed on each material. The fracture toughness (K_{IC}) was calculated by the following equation [36,37]:

$$K_{IC} = \delta \left(\frac{E}{H}\right)^{1/2} \frac{P}{C^{3/2}}$$

where E is the elastic modulus (240 GPa for zircon), H is the Vickers hardness, P is the indentation test load, C is the

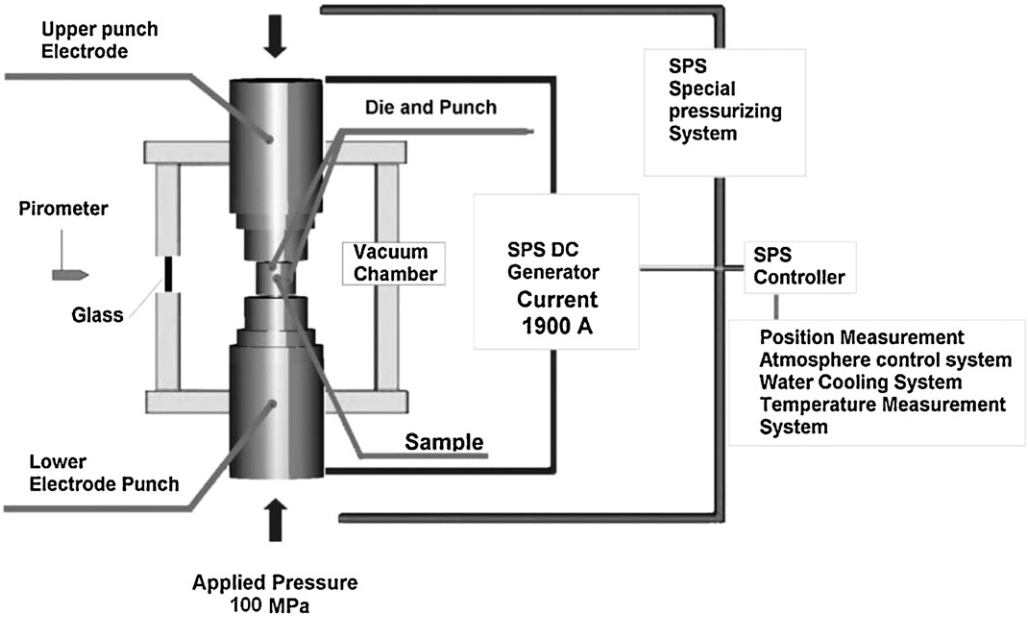

Fig. 1. Schematic diagram of SPS apparatus.

averaged indentation crack length and finally δ is a material-dependent constant that was assumed to be 0.018.

3. Results and discussion

Fig. 2A shows the SEM image of the as received zircon powder, sharp edges and grain sizes between 3 or 4 μm and 0.1 μm are evidenced. Fig. 2B and C shows the powder after 60 and 120 min of HEBM respectively. After the milling process, the particles were more rounded and no significant change in the particle size was detected. After 120 min milling, the mean particle size seems larger than the one treated for 60 min. This phenomenon was attributed to agglomeration and cementation occurring during long milling periods. Thus, intermediate milling treatment of 60 min was selected for the powder consolidation.

Fig. 3 shows the apparent particle size distribution of the powders after 60 and 120 min of HEBM (Z60 and Z120 respectively). And these are compared with the as received powder (Z0). Although no significant particle size change was observed, it is clearly shown in this figure that Z0 and Z60 present equivalent particle size distributions, with the only difference in the amount of particles with apparent size below 0.5 μm: the as received material presented around 5% while the milled powders presented less than 2% of this fine fraction.

On the other hand, the Z120 PSD is slightly higher than the other two analyzed powders, showing that in the long term pre-treatment an agglomeration process was initiated: that is the principal reason why this treatment was discarded.

Fig. 4 compares the XRD patterns of the powders before and after the HEBM. Regardless the milling time, all the observed diffraction peaks belong(s) to the zircon phase. As expected, by extending the HEBM time, the diffraction peaks broadening occurred (inset Fig. 4). No amorphization occurred. The grains shape after the HEBM shows significant changes in the morphology if compared with the original powder.

3.1. SPS sintering

The 60 min milled zircon powder was heated at the high heating rate of 100 °C/min up to preset sintering temperatures ranging between 1200 °C and 1500 °C. The 100 MPa pressure was raised after the beginning of the holding time. The pressure was applied gradually at the rate of 3 MPa/s for all the samples. Depending on the sintering temperatures 1200 °C, 1300 °C,

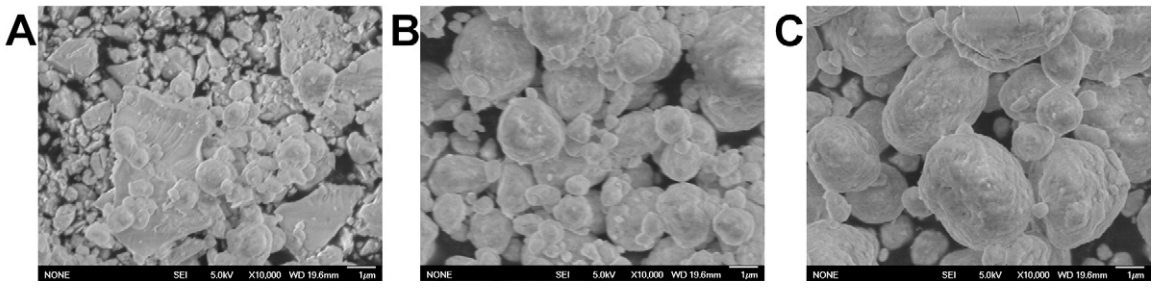

Fig. 2. SEM image of the zircon powders; (A) starting powder, (B) zircon powder after 60 min of HEBM and (C) zircon powder after 120 min of HEBM.

Please cite this article in press as: N.M. Rendtorff, et al., Dense zircon ($ZrSiO_4$) ceramics by high energy ball milling and spark plasma sintering, Ceram. Int. (2011), doi:10.1016/j.ceramint.2011.10.001

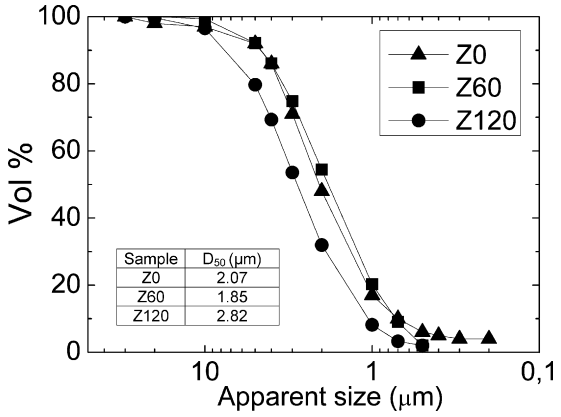

Fig. 3. Apparent particle size distribution of the zircon powders before and after different HEBM pretreatments.

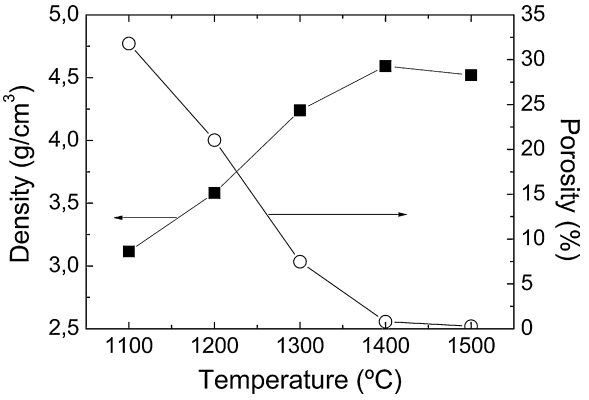

Fig. 5. Density and apparent porosity as a function of the sintering temperature (10 min of dwell time).

1400 °C and 1500 °C the samples were named as S12, S13, S14 and S15 respectively.

The as received zircon powder was sintered under the identical temperature and pressure conditions. However, we could not achieve a satisfactory level of compaction for quantitative analysis. The resulting compacts lacked of sinterization, and lost integrity after the SPS treatment. Hence, no further characterization was carried out on the unmilled powders; the HEBM pretreatment was effective to obtain dense and additive-free zircon ceramics.

The effect of the sintering temperature on the final density and the apparent porosity is plotted in Fig. 5. As expected, the density increased with the temperature. The density of sample S14, sintered at 1400 °C, approaching the theoretical density of zircon (i.e. porosity was less than 1%). The S15 (1500 °C) density was slightly lower: this was attributed to the zircon dissociation as described in Section 3.2.

The nearly fully dense ceramic obtained without sintering additives by HEMB followed by low temperature SPS represents an outstanding achievement in the processing of zircon ceramic regarding (i) the manufacturing of the fully dense material without phase decomposition and (ii) the low sintering temperature and short holding time. In fact, by employing conventional sintering methods, fully dense zircon cannot be obtained at a temperature as low as 1400 °C [2,4–8,10]. Shi et al. [6,15] obtained fully dense zircon material by hot pressing at 1600 °C for 1 h under 25 MPa. However residual open porosity of 5% was achieved without full densification by pressure less sintering [5].

3.2. Phases composition

Fig. 6 shows the diffraction patterns of the sintered materials (the patterns were vertically shifted for easy comparison). The only crystalline phase that can be detected in the S12, S13 and S14 materials is zircon. However, S15 contains zircon, and monoclinic zirconia (Badeyellite). The inset of Fig. 5 shows the main diffraction peaks of monoclinic phase, the tetragonal zirconia peak at $2\theta \approx 30^{\circ}$ was barely detected as well. At 1500 °C the partial dissociation of the zircon into zirconia and silica explains the decrease in the density as shown in Fig. 4. The zircon dissociation occurs at 1675 °C [22], however, as mentioned the presence of impurities lower the dissociation temperature. The electric field generated by the SPS did not influence the dissociation process since the zircon material behaved essentially as an electric insulator during the sintering. Consequently, the zircon decomposition at 1500 °C was mainly attributed to the impurities contained in the starting powders.

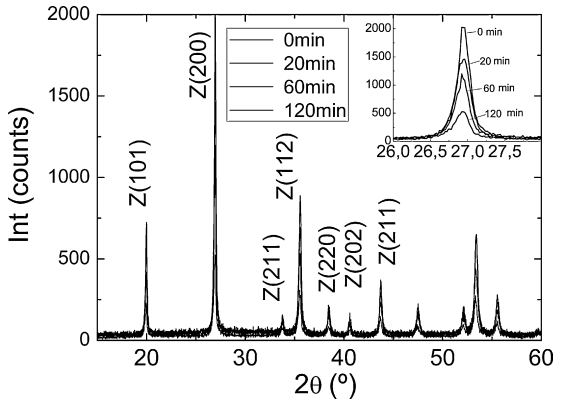

Fig. 4. XRD patterns of the zircon powder before and after different HEBM pretreatments.

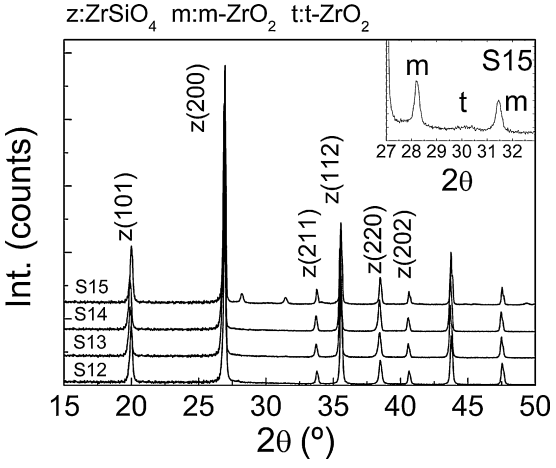

Fig. 6. XRD patterns of the sintered samples.

Please cite this article in press as: N.M. Rendtorff, et al., Dense zircon ($ZrSiO_4$) ceramics by high energy ball milling and spark plasma sintering, Ceram. Int. (2011), doi:10.1016/j.ceramint.2011.10.001

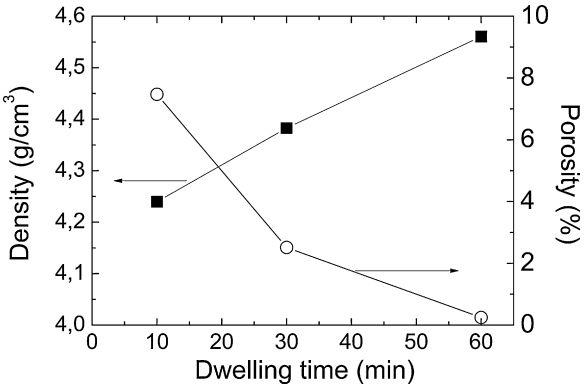

Fig. 7. Density and apparent porosity as a function of the dwell time at 1300 °C and 100 MPa.

Table 1
Effect of SPS processing parameters on the hardness (Hv) and the fracture toughness (K_{IC}) of zircon materials.

Sample	Temperature (°C)	Dwell time (min)	Hv (GPa)	K_{IC} (MPa m$^{-0.5}$)
Maximum temperature effect				
S12	1200	10	3.30 ± 0.03	–
S13	1300	10	5.55 ± 0.04	–
S14	1400	10	13.67 ± 0.09	3.3 ± 0.2
S15	1500	10	11.39 ± 0.08	3.6 ± 0.2
Dwell time effect				
S13	1300	10	5.60 ± 0.04	–
S13-30	1300	30	12.20 ± 0.20	2.5 ± 0.2
S13-60	1300	60	13.90 ± 0.50	2.2 ± 0.2

In order to avoid the zircon dissociation by lowering the sintering temperature, the influence of the holding time was also investigated. The samples S13-30 and S13-60 holding time were 30 and 60 min respectively. Fig. 7 shows the holding time effect on the density/porosity of sintered samples at 1300 °C. No zirconia was detected by XRD or by SEM. By extending the dwell time to 10, 30, 60 min the porosity decreased down to 8.3 and 0.2% respectively.

Fig. 8A–C shows the typical SEM micrographs the samples S14, S15 and S13-60 respectively. The polished surface of S14 and S13-30 samples was thermal etched at 1200 °C for 1 h in an electric kiln.

Even if some close porosity (dark area) can be observed in Fig. 8A, the sample S14 appeared highly densified. The grain size was comparable the starting milled powders (≤3 μm) and no significant grain growth was observed. The rounded morphology, induced by HEBM to the powders was also maintained after sintering.

Fig. 8B shows the typical microstructure of the sample S15. Highly dense bulk zircon ceramic was achieved; however, the thermal dissociation of some zircon grains occurred. The white zirconia area can be observed in the gray zircon matrix. The zirconia resulting from the dissociation did not have a defined shape and its size was comparable to the zircon grains. The zirconia was preferentially dissociated at the zircon–zircon interfaces where the impurities accumulated during the high temperature processing [22,23]. The other product of zircon dissociation, the silica, can be observed in the increment of the thickness of the zircon boundaries (dark gray, in Fig. 8B). Certain amount of m-ZrO_2 was detected by XRD (Fig. 6) but the silica was not detected. The local EDAX analysis confirmed the identification of the three regions (zircon, zirconia and glassy grain boundary).

Fig. 8C shows the well defined grain boundary of dense monophase zircon material obtained after 60 min of dwelling at 1300 °C under uniaxial pressure 100 MPa. This density level cannot be achieved by conventional sintering techniques.

3.3. Hardness and fracture toughness

Hardness together with fracture toughness values are listed in Table 1. As expected, the hardness values increased with the sintering temperature, reaching maximum value for the sample sintered 1400 °C. The hardness of sample S14 is about 40% higher than the values reported for zircon ceramics obtained by HP at 1600 °C [6,15]. The sample S15, due to zircon partial thermal dissociation and the formation of glassy phase resulted in a decrease of the hardness. Due to the difficulties in measuring the crack length on the porous surface, the toughness was not evaluated in the case of S12 and S13. On the other hand the K_{IC} values obtained for both S14 and S15 were higher than the one reported in literature for pure zircon materials. The slightly higher toughness of sample S15 compared to S14 can be addressed to the presence of zirconia which enhances several toughening mechanisms [24–26].

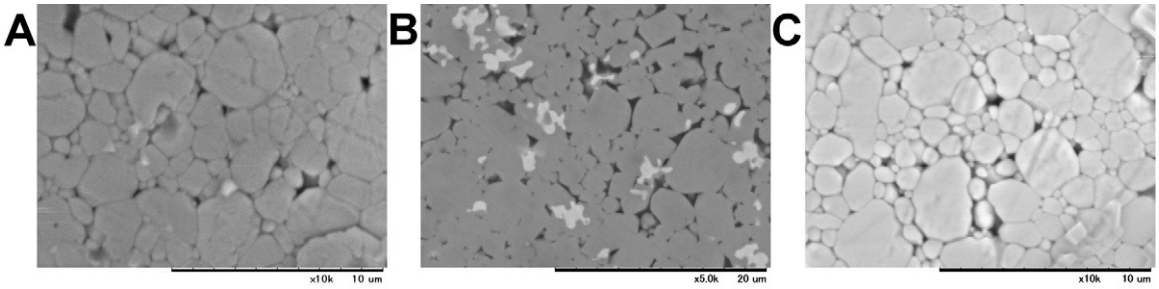

Fig. 8. SEM micrographs of the obtained materials under 100 MPa uniaxial pressure; (A) S14 sample sintered at 1400 °C for 10 min. (B) S15 sample sintered at 1500 °C for 10 min (zircon dissociation is evidenced). (C) S13-60 sample sintered at 1300 °C for 60 min.

Please cite this article in press as: N.M. Rendtorff, et al., Dense zircon ($ZrSiO_4$) ceramics by high energy ball milling and spark plasma sintering, Ceram. Int. (2011), doi:10.1016/j.ceramint.2011.10.001

Table 2
Comparison of material properties with the data reported in the literature.

Method	Maximum temperature; holding time; pressure	Relative density	Hv (GPa)	K_{IC} (MPa $m^{-0.5}$)	Dissociation
Pressure less sintering without sintering additives [5,7]	1600 °C; 2–48 h; pressureless	95%	–	2.2–2.8	Yes
Pressure less sintering with sintering additives [8,9]	1500 °C; 1 h; pressureless	90–95%	11–12	–	Yes
Sintered from pure amorphous SiO_2–ZrO_2 [17]	1500 °C; 4 h; pressureless	99.7	–	–	Complete formation
Hot pressing of pure zircon powders obtained by sol–gel without sintering additives [6]	1600 °C; 1 h; 25 MPa	99.1	10	3.0	No
SPS of high energy milled commercial zircon powder without sintering additives [present study]	1400 °C; 10 min; 100 MPa	≈99.5	11.4–13.7	3.6	No

Finally, by comparing the samples S13-30 and S13-60 (sintered at 1300 °C for 30 and 60 min respectively) with sample S14 (sintered at 1400 °C for 10 min), the low level of porosity as shown in Fig. 7A and C corresponded to high hardness. The grain size and the final density of both dense monophasic materials S14 and S13-60 did not differ significantly. However the fracture toughness evaluated by the indentation technique presented a significant dependence on the holding time and sintering temperature. Typically the fracture toughness of zircon ceramics is ranged between 2.0 and 3.0 MPa $m^{-0.5}$ (Table 2). The K_{IC} for S13-60 is in the low boundary of zircon materials, while the sample S14 exceeds the upper limit of this region by 20%. A plausible explanation is addressed to different kind of grain boundary interface conditions between the zircon grains developed during the SPS.

Finally, in Table 2 a comparison between the different zircon materials reported in the literature was done, showing the merits of the material processed in the present study. While resulting density is comparable with the best figures reported, the hardness and fracture toughness achieved was higher than any pure dense zircon material.

4. Conclusions

Dense zircon ceramics were successfully produced with no additives from mechanically activated powders and spark plasma sintering. The HEBM was an effective pre-treatment for obtaining activated and crystalline zircon powders. Fully dense materials were obtained at 1400 °C with a heating rate of 100 °C/min and a 10 min soaking under 100 MPa uniaxial pressure. In the materials processed at 1500 °C, zircon dissociated in monoclinic zirconia and amorphous silica that resulted in a decrease in the mechanical properties.

Dense materials were also obtained at 1300 °C with 60 min dwell time. However, the mechanical properties were slightly lower than those obtained at 1400 °C.

The SPS in combination with HEBM offers a unique route to obtain pure fully dense zircon ceramic at low temperature (1300–1400 °C) without thermal dissociation.

References

[1] T. Mori, H. Yamamura, H. Kobayashi, T. Mitamura, Preparation of high-purity $ZrSiO_4$ using sol–gel processing and mechanical properties of the sintered body, J. Am. Ceram. Soc. 75 (9) (1990) 2420–2426.
[2] R. Moreno, J.S. Moya, J. Requena, Slip casting of zircon by using an organic surfactant, Ceram. Int. 17 (1) (1991) 37–40.
[3] L.B. Garrido, E.F. Aglietti, Zircon based ceramics by colloidal processing, Ceram. Int. 27 (5) (2001) 491–499.
[4] N.M. Rendtorff, L.B. Garrido, E.F. Aglietti, Effect of the addition of mullite–zirconia to the thermal shock behavior of zircon materials, Mater. Sci. Eng. A 498 (1–2) (2008) 208–215.
[5] R. Moreno, J.S. Moya, J. Requena, Slip casting of zircon, J. Mater. Sci. Lett. 5 (1986) 127–128.
[6] Y. Shi, X. Huang, D. Yan, Fabrication of hot-pressed zircon ceramics: mechanical properties and microstructure, Ceram. Int. 23 (5) (1997) 457–462.
[7] X. Carbonneau, M. Hamidouche, C. Olagnon, G. Fantozzi, R. Torrecillas, High temperature behavior of a zircon ceramic, Key Eng. Mater. 132–136 (1997) 571–574.
[8] J. De Andres, S. de Aza, J.S. Moya, Effect of TiO_2 additions on the sintering behavior of zircon powders, in: Ceramic Materials and Components for Engines, Proceedings of the Second International Symposium, Luebeck-Travemuende, Germany, (1986), p. 9111.
[9] K.B. Lee, J.B. Kang, Sintering behavior of zircon with SiO_2, Korean J. Mater. Res. 18 (11) (2008) 604–609.
[10] K.B. Lee, S.H. Jung, J.S. Lee, G.P. Hong, B.R. Jo, J.S. Moon, J.B. Kang, Effect of SiO_2, Al_2O_3, and clay additions on the sintering characteristics of zircon, Korean J. Mater. Res. 18 (7) (2008) 352–356.
[11] H. Kobayashi, T. Takano, T. Mori, H. Yamamura, T. Mitamura, Preparation of $ZrSiO_4$ powder using sol–gel process (Part 1). Influence of starting materials and seeding, J. Ceram. Soc. Jpn. 98 (6) (1990) 567–572.
[12] T. Mori, H. Yamamura, H. Kobayashi, T. Mitamura, Preparation of high-purity $ZrSiO_4$ powder using sol–gel processing and mechanical properties of the sintered body, J. Am. Ceram. Soc. 75 (9) (1992) 2420–2426.
[13] Y. Shi, X.X. Huang, D. Yan, Preparation and characterization of highly pure fine zircon powder, J. Eur. Ceram. Soc. 13 (2) (1992) 113–119.
[14] W.P.C.M. Alahakoon, S.E. Burrows, A.P. Howes, B.S.B. Karunaratne, M.E. Smith, R. Dobedoe, Fully densified zircon co-doped with iron and aluminium prepared by sol–gel processing, J. Eur. Ceram. Soc. 30 (12) (2010) 2515–2523.
[15] Y. Shi, X. Huang, D. Yan, TEM and SEM characterization of hot-pressed zircon ceramics, Mater. Lett. 23 (1995) 247–252.
[16] P. Tartaj, J. Sanz, C.J. Serna, M. Ocana, Zircon formation from amorphous spherical $ZrSiO_4$ particles obtained by hydrolysis of aerosols, J. Mater. Sci. 29 (24) (1994) 6533–6538.

Please cite this article in press as: N.M. Rendtorff, et al., Dense zircon ($ZrSiO_4$) ceramics by high energy ball milling and spark plasma sintering, Ceram. Int. (2011), doi:10.1016/j.ceramint.2011.10.001

[17] P. Tartaj, Zircon formation from nanosized powders obtained by a reverse micelle process, J. Am. Ceram. Soc. 88 (1) (2005) 222–224.
[18] P. Tartaj, L.C. De Jonghe, Preparation of nanospherical amorphous zircon powders by a microemulsion-mediated process, J. Mater. Chem. 10 (12) (2000) 2786–2790.
[19] R.C. Garvie, Improved thermal shock resistant refractories from plasma-dissociated zircon, J. Mater. Sci. 14 (1979) 817–822.
[20] P. Taraj, C.J. Serna, J.S. Moya, J. Requena, M. Ocaña, S. De Aza, F. Guitian, The formation of zircon from amorphous ZrO_2SiO_2 powders, J. Mater. Sci. 31 (1996) 6089–6094.
[21] S. Schelz, F. Enguehard, N. Caron, D. Plessis, B. Minot, F. Guillet, J. Longuet, N. Teneze, E. Bruneton, Recombination of silica and zirconia into zircon by means of laser treatment of plasma-sprayed coatings, J. Mater. Sci. 43 (2008) 1948–1957.
[22] A. Kaiser, M. Lobert, R. Telle, Thermal stability of zircon ($ZrSiO_4$), J. Eur. Ceram. Soc. 28 (2008) 2199–2211.
[23] P. Pena, S. De Aza, The zircon thermal behaviour: effect of impurities, J. Mater. Sci. 19 (135) (1984) C42.
[24] H. Zender, H. Leistner, H. Searle, ZrO_2 Materials for applications in the ceramic industry, Interceramics 39 (6) (1990) 33–36.
[25] P.M. Kelly, L.R. Francis Rose, The martensitic transformation in ceramics its role in transformation toughening, Prog. Mater. Sci. 47 (5) (2002) 463, C557.
[26] X. Jin, Martensitic transformation in zirconia containing ceramics and its applications, Curr. Opin. Solid State Mater. Sci. 9 (6) (2005) 313, C318.
[27] C. Suryanarayana, Mechanical alloying and milling, Prog. Mater. Sci. 46 (1–2) (2001) 1–184.
[28] V.N. Antsiferov, V.B. Kulmeteva, S.E. Porozova, B.L. Krasnyi, V.P. Tarasovskii, A.B. Krasnyi, Application of mechanochemical activation in production of zircon ceramics, Russ. J. Non-Ferrous Met. 51 (2) (2010) 182–187.
[29] D.R. Spearing, J.Y. Huang, Zircon synthesis via sintering of milled SiO_2 and ZrO_2, J. Am. Ceram. Soc. 81 (7) (1998) 1964–1966.
[30] M. Omori, Sintering, consolidation, reaction and crystal growth by the spark plasma system (SPS), Mater. Sci. Eng. A 287 (2) (2000) 183–188.
[31] R. Orru, R. Licheri, A.M. Locci, A. Cincotti, G. Cao, Consolidation/synthesis of materials by electric current activated/assisted sintering, Mater. Sci. Eng. R: Rep. 63 (4–6) (2009) 127–287.
[32] S. Grasso, Y. Sakka, G. Maizza, Electric current activated/assisted sintering (ECAS): a review of patents 1906/2008, Sci. Technol. Adv. Mater. 10 (2009) 053001.
[33] K. Morita, K. Hiraga, B.N. Kim, H. Yoshida, Y. Sakka, Synthesis of dense nanocrystalline ZrO_2–$MgAl_2O_4$ spinel composite, Scr. Mater. 53 (9) (2005) 1007–1012.
[34] G. Suárez, Y. Sakka, T.S. Suzuki, T. Uchikoshi, X. Zhu, E.F. Aglietti, Effect of starting powders on the sintering of nanostructured ZrO_2 ceramics by colloidal processing, Sci. Technol. Adv. Mater. 10 (2009) 025004.
[35] T. Shimonosono, H. Kimura, Y. Sakka, Effect of grain size on electrical properties of scandia-stabilized zirconia, J. Ceram. Soc. Jpn. 118 (2010) 1038–1043.
[36] H. Miyazaki, H. Hyuga, Y. Yoshizawa, K. Hirao, T. Ohji, Measurement of indentation fracture toughness of silicon nitride ceramics: I, effect of microstructure of materials, Key Eng. Mater. 352 (2007) 41–44.
[37] K. Niihara, R. Morena, D.P.H. Hasselman, Evaluation of K_{IC} of brittle solids by the indentation method with low crack-to-indent ratios, J. Mater. Sci. Lett. 1 (1982) 13–16.

Please cite this article in press as: N.M. Rendtorff, et al., Dense zircon ($ZrSiO_4$) ceramics by high energy ball milling and spark plasma sintering, Ceram. Int. (2011), doi:10.1016/j.ceramint.2011.10.001